ERROR BOUNDS FOR
GENERAL DESCRIBING FUNCTION PROBLEMS

by

A. R. Bergen, L. O. Chua and A. I. Mees

and E. W. Szeto

Memorandum No. UCB/ERL M81/55

16 July 1981

ELECTRONICS RESEARCH LABORATORY

College of Engineering
University of California, Berkeley
94720

Error Bounds for General Describing Function Problems*

A. R. Bergen, L. O. Chua, A. I. Mees and E. W. Szeto†

Abstract

The describing function method is widely used without much attention being paid to the error analysis so vital in any approximate method. One reason for this is the lack of a straightforward, user-oriented method for checking error bounds except when the nonlinear element characteristic is single value and of bounded slope. This paper attempts to eliminate that defect. A far wider range of nonlinear elements is now amenable to straightforward, usually graphical treatment; discontinuities, hysteresis and backlash characteristics are included. In addition, previous results for slope-bounded single-valued nonlinear characteristics may be substantially improved with a small additional computational effort.

*This paper is supported in part by the Office of Naval Research under contract N00014-76-C-0572, the National Science Foundation Grants ENG77-22745/ ECS-8020640 and by the Department of Energy contract DE-AC01-79-ET29364.

†A. R, Bergen, L. O. Chua and E. W. Szeto are with the Department of Electrical Engineering and Computer Sciences and the Electronics Research Laboratory, University of California, Berkeley, CA 94720.

A. I. Mees is with the Department of Pure Mathematics and Mathematical Statistics, Cambridge University, 16 Mill Lane, Cambridge CB2 1SB, England.

1. Introduction

The describing function method is the first order version of the method of harmonic balance, which tries to find periodic solutions for nonlinear systems by fitting a truncated Fourier series. Traditionally, the method addresses itself to the system of Fig. 1.1, and the solution is found using graphical constructions involving the Nyquist locus. The tradition has not died out with the universal availability of computers; rather, it has been strengthened because of the vastly more informative nature of graphic displays over lists of numbers. In addition, the use of the Nyquist locus (or the inverse Nyquist locus, which we prefer for error analysis) makes it easier to link the problem with the question of larger system design or analysis, of which it is usually a part.

Of course, the describing function method is approximate and a lot of work has been put into error analysis, from Bass's early studies [1] and the general theory of Cesari [2] through the detailed investigations in the early 1970's [3,4,5,6,7] to the recent revival of interest [8,9,10]. It seems to the present authors that this work should be made more accessible to anyone who uses describing functions. We feel that previous work has either been too difficult for use by non-experts, or has only been available for a restricted set of nonlinear elements.

This paper sets out to remedy this, by providing a set of graphically oriented tools that are described in a purely operational manner in section 2. Several examples are given in section 3. The theory presented in section 4 draws on much of the literature referenced above (particularly the work of Michel and Miller [8] who considered the non-autonomous version of the same problem), but it contains novel features and we have taken care to direct it towards graphical interpretations. The principal novel feature is the use of a combination of L_2 and L_∞ norms in a way that allows us to restrict attention to only part of the domain of the nonlinear element, which in turn allows new problems to be solved and tightens bounds on the old ones. Another novel feature is the use of an amplitude and frequency-dependent poleshift to optimize the error estimate. By taking advantage of all the optimizations, a very tight error bound can usually be obtained, but there is also the option of obtaining a less precise bound with less effort by doing less optimization and by using easily-obtained upper bounds on the various functions.

2. How to use the results

We shall now explain the method of calculating error bounds in almost a cook-book fashion. A minimal amount of theory will be introduced, and the main

body is postponed until section 4.

The idea is to find Ω, a set of fundamental frequency and amplitude values, (ω,a_1), that can be shown to contain the fundamental frequency and amplitude of a true oscillatory solution to the system in Fig. 1.1. As shown in section 3, we find this set Ω by defining various functions p, q and r needed to state a key inequality at all points in Ω.

We assume that the autonomous single-loop feedback system of Fig. 1.1 has a linear part g with a transfer function $G(j\omega)$, and a nonlinear part n having a describing function $N(a_1)$. The nonlinear element may be multivalued and discontinuous; the very mild restrictions on its behavior are that $N(\cdot)$ must be continuous over the set of a_1 values of interest and that over the domain of inputs of interest, the given nonlinear input-output relation can be approximated in an arbitrarily close fashion by a slope-bounded, though possibly multivalued function or relation.[1] All of the usual relay-type elements satisfy these conditions.

We assume the first order describing function equations

$$N(a_1) + \frac{1}{G(j\omega)} = 0 \qquad (2.1)$$

have a solution $(\hat{\omega},\hat{a}_1)$. We are trying to verify that this corresponds to a true oscillatory solution to the system equations, and if so, to find intervals containing its frequency and fundamental amplitude. We will now describe the steps needed to do this, introducing notation as required. A relatively simple version of the procedure is summarized in Table 1, and it may be helpful to scan the table now, and to consult it later when working out examples or following through the theory. Table 2 shows the full version, which usually has to be done using a (small) computer.

2.1. Preliminaries

We decide whether we are looking for π-symmetric solutions (those containing only odd harmonics) or more general ones. If we are looking for π-symmetric solutions -- so that n must be an odd function or relation -- we define

$$K = \{1,3,5,\ldots\} \quad \text{and} \quad K^* = \{3,5,\ldots\} \ .$$

[1] Whenever we deal with multivalued functions or relations, we must have a rule for uniquely selecting the output produced by any given periodic input.

If we are looking for more general 2π-symmetric solutions, we define

$$K = \{0,1,2,3,\ldots\}$$

and then we decide what to do with the bias term. It can be solved for separately [10,11] in which case

$$K^* = \{2,3,4,\ldots\} \ ;$$

or it can be neglected just like the high harmonics, in which case

$$K^* = \{0,2,3,4,\ldots\} \ .$$

We now introduce some notation. If $x(t)$ is a 2π-periodic function of period $2\pi/\omega$, by a suitable time normalization we can pick $\omega = 1$ and we write

$$x(t) = \text{Re} \sum_{k\in K} a_k \, e^{jkt}$$

and

$$x^*(t) = \text{Re} \sum_{k\in K^*} a_k \, e^{jkt}$$

Thus, x^* is the part of the solution that was neglected when we obtained the describing function estimate of the solution. We expect reliable results only if x^* is sufficiently small.

Now we calculate how well the linear part of the system filters out unwanted harmonics; the filtering effect is the usual justification for assuming x^* is small. Define

$$\rho(\omega) = \sqrt{\sum_{k\in K^*} |G(jk\omega)|^2} \ .$$

Notice that the sum will converge if $|G(s)|$ is $o\left(\left|\frac{1}{s}\right|^m\right)$ with $m > \frac{1}{2}$, as $\left|\frac{1}{s}\right| \to 0$. In practice, G is usually strictly proper and the convergence is very fast, so only a few terms are needed to get a very good estimate of $\rho(\omega)$. Small values of $\rho(\omega)$ are desirable; the smaller ρ is, the better the eventual error estimate.

The next step is to find the describing function output error -- that is, the error in assuming that the output of n is sinusoidal when its input is sinusoidal. The function required is

$$p(a_1) = \sqrt{\|n(a_1 \cos t)\|_2^2 - |a_1 N(a_1)|^2}$$

where the L_2 norm on $[0, 2\pi]$ is $\|\cdot\|_2$, defined by

$$\|f(t)\|_2^2 = \frac{1}{\pi}\int_0^{2\pi} f(t)^2\, dt\ .$$

The function $p(a_1)$ can always be calculated explicitly, but if n has finite gain β (i.e. $|n(x)| \leq \beta|x|$ for all x in the region of interest) then, with some loss of accuracy in the eventual error estimate, we can replace $p(a_1)$ by an upper bound βa_1. Incidentally, we shall see later that it is sometimes possible to get by without calculating p. The crucial step is to calculate a function that measures the error introduced by neglecting high harmonics at the <u>input</u> of n. The function is defined using the sup norm

$$\|f(t)\|_\infty = \sup_{t\in[0,2\pi]} |f(t)|\ ,$$

and uses an upper bound ε on $\|x^*\|_\infty$, the sup norm of the neglected (usually higher) harmonics. The function is

$$q(a_1,\varepsilon) = \sup_{\|x^*\|_\infty\leq\varepsilon} \|n(a_1\cos t + x^*(t)) - n(a_1\cos t)\|_2$$

Take careful note of the <u>two different norms</u> used here. The actual calculation of q is by a worst-case analysis of the integral involved in the L_2 norm. If n is single-valued, we can define

$$m(x,\varepsilon) = \sup_{|y-x|\leq\varepsilon} |n(y)-n(x)|\ ,$$

so that

$$q(a_1,\varepsilon) = \sqrt{\frac{1}{\pi}\int_0^{2\pi} m(a_1\cos t\ ,\varepsilon)^2 dt}\ .$$

(For example, if $n(x) = \operatorname{sgn} x$, then $m(x,\varepsilon) = 2$ when $|x| \leq \varepsilon$ and $m(x,\varepsilon) = 0$ when $|x| > \varepsilon$. This leads to $q(a_1,\varepsilon) = 4\sqrt{\frac{1}{\pi}\sin^{-1}(\frac{\varepsilon}{a_1})}$. If n is many-valued, we need different functions m when x is increasing and when it is decreasing, but otherwise the calculation is similar.

If n has slope bound λ, then $m(x) \leq \lambda\varepsilon$ for all x, so q may be replaced by an upper bound $\sqrt{2}\ \lambda\varepsilon$, although the more detailed calculation will usually lead to a smaller value. The smaller the value of q, the better the eventual error estimate.

2.2. Finding the set Ω

With ρ, p and q known, the rest of the process involves solving an equation to find an upper bound on the higher harmonic error, ε, then finding a set Ω of (ω,a_1) values that satisfy a key inequality, and finally checking a non-degeneracy condition which is nearly always trivially satisfied.

To find a suitable value of ε, we have to satisfy the inequality

$$\rho(\omega)\ \min\{q(a_1,\varepsilon) + p(a_1),\ r(a_1,\varepsilon)\} \le \varepsilon \qquad (2.2)$$

where

$$r(a_1,\varepsilon) = \sqrt{2} \sup_{|y|\le a_1+\varepsilon} |n(y)| \ .$$

This inequality has to hold for some $\varepsilon(\omega,a_1) > 0$ for all $(\omega,a_1) \in \Omega$. In fact we do not know Ω yet. All we know at this stage is that $(\hat{\omega},\hat{a}_1) \in \Omega$ where $(\hat{\omega},\hat{a}_1)$ is the describing function solution. In practice, we proceed as follows. Find the smallest ε which satisfies (2.2) for $(\omega,a_1) = (\hat{\omega},\hat{a}_1)$. We can then guess a larger value of ε, check that it still satisfies inequality (2.2) for $(\hat{\omega},\hat{a}_1)$, and later, complete the check when Ω is known.

Alternatively, we can try to solve (2.2) as an implicit equation: for each given pair of values of ω and a_1, we look for the smallest positive ε for which there is an intersection between the line $y = \varepsilon$ and the curve

$$y = f(\varepsilon) \triangleq \rho(\omega)\ \min\{q(a_1,\varepsilon) + p(a_1),\ r(a_1,\varepsilon)\} \ .$$

Since q and r are both monotone increasing functions of ε, if there are any intersections between the line and the curve, the first intersection will be found by applying the contraction mapping theorem to find a fixed point of $f(\varepsilon)$, starting from $\varepsilon = 0$. In this way we can find the smallest ε for each ω and a_1.

Because of the term $r(a_1,\varepsilon)$, any nonlinear element that saturates (or, more generally, any nonlinear element that eventually grows slower than linearly) will produce a finite value of ε. In section 2.3, we will show how the value of ε can, if required, be minimized. In general, though, it is possible that no solution exists to (2.2), either because the linear part is not a good enough filter or the nonlinear part is badly behaved. In such a case, we can go no further with this method. Pole-shifting may save the day by reducing the values of q and p: this is discussed in section 2.3.

We now try to find a closed bounded set Ω that contains $(\hat{\omega},\hat{a}_1)$ and all nearby points that satisfy the key inequality

$$|N(a_1) + \frac{1}{G(j\omega)}| \leq \sigma(\omega,a_1) \tag{2.3}$$

where

$$\sigma(\omega,a_1) = q(a,\varepsilon(\omega,a_1))/a_1 \tag{2.4}$$

with $\varepsilon > 0$ satisfying (2.2); the tightest bounds are found using the smallest values of ε. There are three ways of finding Ω; the first provides the smallest set, but requires more work than the other two. If no bounded Ω can be found, the error analysis has failed.

(a) We can find Ω directly as described in reference [4]: surround $(\hat{\omega},\hat{a}_1)$ by a grid of points and at each point, find ε and calculate the ratio:

$$\frac{N(a_1)+\frac{1}{G(j\omega)}}{\sigma(\omega,a_1)} \quad .$$

The boundary of Ω consists of those points where the ratio is 1.

(b) We can fix ε at some slightly pessimistic (large) value and use the inequality (2.3). This is easy to implement graphically since it says that points (ω,a_1) inside Ω must be such that the distance between $N(a_1)$ and $-1/G(j\omega)$ is at most $q(a_1,\varepsilon)/a_1$. Consequently, we can choose a range of a_1 values, and draw discs centered on $N(a_1)$ and of radius $q(a_1,\varepsilon)/a_1$. The envelope of the discs cuts off a range of ω values and the first and last discs to intersect the $-1/G$ locus define the correct a_1 range (see Fig. 2.1). This is analogous to the discs drawn on the $-1/G$ locus in reference [6]. We obtain a rectangle $[\omega_{min}, \omega_{max}] \times [a_{1_{min}}, a_{1_{max}}]$ which will contain the set Ω found in method (a), and we check that the ε we fixed is actually big enough over this rectangle.

(c) We can select a range A of a_1 values and find the maximum of $\sigma(\omega,a_1)$ over that range. This gives an inequality involving only frequency on the right side:

$$|N(a_1) + \frac{1}{G(j\omega)}| \leq \sup_{a_1 \in A} \sigma(\omega,a_1) \ .$$

(Even if ε has been fixed to simplify the calculation, we can still do this by using σ' instead of σ, where

$$\sigma'(\omega,a_1) = \frac{\left(\frac{\varepsilon}{p(\omega)} - p(a_1)\right)}{a_1} \quad .$$

This results from combining (2.2) and (2.4)}. Now we can draw discs on the locus of -1/G, but otherwise proceed as in method (b). A justification and verification of using error circles this way will be exemplified in Example 3.1.

The final step in the error analysis is to check for nondegeneracy of the intersection between the loci of N and -1/G. "Non-degeneracy" here means nonzero degree relative to Ω (see sec. 4) and if method (a) is used to find Ω, we merely calculate the degree d from its definition:

$$d(N+\frac{1}{G}\ ,\ \Omega,\ 0) = \sum_i \operatorname{sgn}(\det J_i) \quad .$$

The summation is over all describing function solutions in Ω, and J_i is the derivative matrix at the ith solution,

$$J_i = \begin{bmatrix} \frac{\partial f_1}{\partial \omega} & \frac{\partial f_1}{\partial a_1} \\ \frac{\partial f_2}{\partial \omega} & \frac{\partial f_2}{\partial a_1} \end{bmatrix}$$

where f_1 and f_2 are the real and imaginary parts of N + 1/G. If any J_i is singular, the system must be perturbed slightly to make it nonsingular before d is found. The perturbation must not move any solution over the boundary of Ω.

If method (b) or (c) is used, the degree can be calculated by inspection. Imagine the N and -1/G loci to be made of string, and put pegs at the points $N(a_{1_{min}})$, $N(a_{1_{max}})$, $-1/G(j\omega_{min})$, $-1/G(j\omega_{max})$. Now pull the strings taut from outside the pegs, without allowing any string to jump over a peg. If the strings still cross, the degree is non-zero (see Fig. 2.2). If the strings do not cross, the degree is zero and the error analysis has failed.[2] If all is well up to this stage, we are done: there is at least one oscillatory solution $a_1\cos\omega t + x^*(\omega t)$ with $(\omega,a_1) \in \Omega$ and $\|x^*\|_\infty \leq \varepsilon$.

[2]For a more technical explanation of the calculation of the degree, the interested reader should consult reference [12]. Also, reference [13] (section 2.1) contains a compact treatment of degree theory treated from a circuit-theoretic viewpoint.

2.3. Poleshifting

It is well-known that pole-shifting is extremely helpful in analyzing nonlinear feedback systems. In an earlier paper, two of the authors used pole-shifting to give good results in cases where the nonlinear element is slope-bounded [6]. Here, we extend this idea a good deal further by introducing two different poleshift factors, each of which may be chosen to depend on frequency and amplitude if desired, so as to optimize the size of the error estimates.

In section 4, we will justify the method described here. For any $\gamma \in \mathbb{R}$, we write

$$\tilde{n}(x,\gamma) = n(x) - \gamma x$$

and we define $\tilde{q}(a_1,\varepsilon,\gamma)$ exactly as we defined $q(a_1,\varepsilon)$, except that $\tilde{n}$ is used instead of n:

$$\tilde{q}(a_1,\varepsilon,\gamma) = \sup_{\|x^*\|_\infty \leq \varepsilon} \|n(a_1\cos t + x^*) - n(a_1\cos t) - \gamma x^*\|_2 \quad .$$

The definitions of p and r remain unchanged, but now we have

$$\tilde{\rho}(\omega,\gamma) = \sum_{k\in K^*} \left| \frac{G(j\omega)}{(1+\gamma G(jk\omega))} \right|^2 \quad .$$

Let $\tilde{\varepsilon}(\omega,a_1,\gamma)$ be the smallest positive solution of

$$\varepsilon = \tilde{\rho}(\omega,\gamma)\ \min\{p(a_1) + \tilde{q}(a_1,\varepsilon,\gamma),\ r(a_1,\varepsilon)\} \qquad (2.5)$$

We can choose γ to minimize $\tilde{\varepsilon}$. This is a one-dimensional optimization problem and is therefore easily solved: in the examples later, we have chosen to solve (2.5) by contraction mapping and to find γ by the "Golden section method" [14], merely because this approach is sufficiently reliable and trivially easy to program. However, the problem is best described as the two-dimensional optimization problem:

minimize ε,

subject to $\varepsilon \geq 0$, $\gamma \in \mathbb{R}$ and

$$\varepsilon \geq \tilde{\rho}\ (\omega,\gamma)\ \min\ \{p(a_1) + \tilde{q}(a_1,\varepsilon,\gamma)\ ,\ r(a_1,\varepsilon)\}\ ,$$

which can be solved numerically in negligible time by any of the standard methods.

Having obtained $\varepsilon(\omega,a_1) = \min_{\gamma} \tilde{\varepsilon}(\omega,a_1,\gamma)$, we can choose a different γ, if desired, to minimize

$$\tilde{\sigma}(\omega,a_1,\gamma) = \frac{\tilde{q}(a_1,\varepsilon(\omega,a_1),\gamma)}{a_1} \quad ,$$

giving, say, $\sigma(\omega,a_1)$, and then proceed to find Ω in the usual way.

We wish to emphasize that the poleshift factor γ is <u>arbitrary</u>. One can use the optimal value of γ, or $\gamma = 0$, or, say, $\gamma = \frac{1}{2}(\alpha+\beta)$ if the nonlinearity n has slope bounds α and β, or any other value. Moreover, it is desirable to optimize if one wants the best bounds, and the optimization can easily be incorporated in a package of computer programs for describing function analysis.

3. <u>Examples</u>

The examples in this section are intended to illustrate the various levels of sophistication to which the error bounding method can be carried out. The first example, dealing with a backlash nonlinearity, is very simple as it uses a slope bound estimate to obtain q and a fixed estimate to obtain ε. Also, no poleshifting is involved and the whole calculation can be done entirely by hand. The second example looks at a Wien bridge oscillator and compares results obtained by an earlier method described in [6] with optimized bounds from the present method. In the third example, we show how to deal with a nonlinear element, $n(x) = x^3$, which does not have global or sector bounds. We solve this problem entirely numerically, with full optimization. The fourth example concerns a relay with deadzone and hysterisis, and it uses the optimization techniques mentioned in the paper. All our numerical calculations have been done on an HP 9845A desk-top computer and the total computer time taken to solve the problems is negligible. Our techniques can easily be implemented on a more versatile system at almost no cost.

<u>Example 3.1</u>.

The backlash nonlinearity shown in Fig. 3.1 has a slope bound of 1 (i.e. $|n(x)-n(y)| \leq |x-y|$ $\forall$ x and y, regardless of history) so we know that $q(a_1,\varepsilon) \leq \varepsilon\sqrt{2}$. (A more careful worst-case analysis would show that the inequality here can be replaced by equality.) The describing function is

$$N(a_1) = \frac{1}{\pi}\left[\frac{\pi}{2} + \sin^{-1}\left(1 - \frac{2}{a_1}\right) + 2\left(1 - \frac{2}{a_1}\right)\left(\frac{1}{a_1} - \frac{1}{a_1^2}\right)^{1/2} - j4\left(\frac{1}{a_1} - \frac{1}{a_1^2}\right)\right] .$$

The function p used in the error analysis is given by

$$p(a_1)^2 = \|n(a_1 \cos t)\|_2^2 - |a_1 N(a_1)|^2$$

$$= \frac{a_1^2}{2} + 2a_1 + 2 + \frac{2}{\pi}\left[\left(\frac{a_1^2}{2} - 2a\right)\psi + \frac{a_1^2}{4}\sin 2\psi + 2a\cos\psi\right],$$

where $\psi = \pi - \sin^{-1}\left(1 - \frac{2}{a_1}\right)$.

Ogata [15] considers a negative feedback system containing this backlash element and the linear element with transfer function $G(s) = \frac{10}{s(s+1)}$. In this case, $\frac{-1}{G(j\omega)} = 0.1\omega^2 - j0.1\omega$ and a rough sketch of the N and -1/G loci reveals an intersection which, on slightly more careful analysis, is found to occur near $\omega = 2.72$ and $a_1 = 3.25$. Evaluating $p(a_1)$ near $a_1 \in [2.8, 3.8]$, we discover that $p(a_1)/a_1 < 0.1$ everywhere.

Since $q(a_1, \varepsilon) \leq \sqrt{2}\,\varepsilon$, we can solve for ε, obtaining

$$\varepsilon \leq \frac{\sqrt{2}\,\rho(\omega)}{1 - \sqrt{2}\,\rho(\omega)}$$

and hence

$$\sigma(\omega, a_1) \leq \frac{\sqrt{2}\,\rho(\omega)}{1 - \sqrt{2}\,\rho(\omega)} \cdot \frac{p(a_1)}{a_1} .$$

Using the bound $p(a_1)/a_1 < 0.1$ and computing $\rho(\omega)$ for a few values of $\omega \in [2.5, 2.8]$, we can draw circles on the -1/G locus as in Fig. 3.2, obtaining the error bounds

$$\omega \in [2.59, 2.80], \quad a_1 \in [2.75, 3.65] .$$

These are relatively coarse bounds -- we could do better by using the methods described in the paper -- but they verify the prediction by the describing function method that the system can oscillate.

Example 3.2.

To compare results obtained by the new method with results obtained by the older method for slope-bounded functions, consider the Wien bridge oscillator in Fig. 3.3a, where the operational amplifier (op amp) is assumed to be ideal.

The circuit can be modeled by the single-loop feedback system of Fig. 1.1 where $n(x)$ is now the ideal op amp characteristic of Fig. 3.3b, and $G(s) = \frac{-s^2+s-1}{4(s^2+3s+1)}$. Note that $n(x)$ is a discontinuous function, which presents no problems for our error analysis. However, G is not strictly proper, so $\rho(\omega)$ is infinite. One way to circumvent this problem is to remove the constant part of G and absorb it into n, i.e., we poleshift n. This gives the model shown in Fig. 3.4, where the gain provided by the 1KΩ and 3kΩ resistors is accounted for by the first feedback loop. A simple analysis shows that this can further be reduced to the equivalent system of Fig. 1.1, with $G'(s) = \frac{-s}{(s^2+3s+1)}$ and $n'(x)$ being the saturation characteristic of Fig. 3.5. Two of the present authors analyzed this circuit by performing a similar transformation on the original circuit [16]. With an arctangent approximation to the saturation nonlinearity, they have used the Hopf bifurcation theorem to predict an oscillation with frequency near 1 and amplitude near 4.

Using the graphical error bound method in [6] for describing functions, we can easily show that there is an oscillation with $\omega \in [0.9, 1.052]$ and $a_1 \in [3.45, 5]$. The error circles (of radius σ) have radii around 0.1. Performing an error analysis on the same circuit using the techniques described in this paper, we have obtained a significant improvement over the previous result. With an optimal poleshift factor of around 1.8, the value of σ is reduced to near 0.05, and there is found to be an exact solution with $\omega \in [0.97, 1.03]$ and $a_1 \in [3.8, 4.2]$.

Of course, it may not be very important to obtain such tight error bounds; but there are many cases -- such as Example 3.3 which follows -- where poor error estimates render it impossible to even obtain a bounded Ω, so it becomes impossible to complete the error analysis. In such cases, the improvements we have described are indispensible.

Example 3.3.

When $n(x) = x^3$ and $G(x) = \frac{(s+1)}{(s^3+2s^2+s+3)}$, the Nyquist locus (of G, and not of -1/G) is shown in Fig. 3.6. Since $N(a_1) = \frac{3}{4} a_1^2$, the locus of -1/N lies along the negative real axis, so there is a describing function solution which turns out to be $\omega = \sqrt{2}$, $a_1 = \sqrt{4/3}$. The intersection is, however, at a fairly shallow angle, and the high harmonic part of the G locus remains close to the -1/N locus and even comes back towards it at high frequencies; so we might suspect

the solution to be inaccurate. If we apply the full error analysis of Table 2, (with $p(a_1) = \frac{1}{4} a_1^3$ and $\tilde{q}$ calculated by numerical integration), we find typical values of ε near 0.05 (with γ around 1), and σ near 0.05 (with γ around 2). The detailed (ω, a_1) picture is shown in Fig. 3.7, with $|N + 1/G|/\sigma \leq 1$ in the shaded set Ω. The result is $a_1 \in [1.10, 1.27]$ and $\omega \in [1.385, 1.47]$, with an upper bound of 0.11 for ε over the whole of Ω. These results are in agreement with higher order harmonic balance computations [5].

Example 3.4.

The hysteretic relay shown in Fig. 3.8 has $r(a_1,\varepsilon) = \sqrt{2}$, so without further effort, we get $\varepsilon \leq \sqrt{2}\, \rho(\omega)$. To find q, we define

$$m(x,\varepsilon) = \begin{cases} 1 \ , & \text{if } x - \varepsilon > \xi \text{ or } -x + \varepsilon < -\eta \\ 0 \ , & \text{otherwise} \end{cases}$$

so q is given by

$$q(a_1,\varepsilon)^2 = \frac{2}{\pi} \int_0^{\pi} m(a_1 \cos t, \varepsilon)^2 \, dt \ .$$

As long as $0 \leq \varepsilon \leq \xi+\eta$ and $a_1 > \eta+\varepsilon$, we have

$$q(a_1,\varepsilon) = \sqrt{\frac{2}{\pi} \left[\sin^{-1} \frac{\xi+\varepsilon}{a_1} - \sin^{-1} \frac{\xi-\varepsilon}{a_1} + \sin^{-1} \frac{\eta+\varepsilon}{a_1} - \sin^{-1} \frac{\eta-\varepsilon}{a_1}\right]} \ .$$

To get some feel for what this means, suppose a_1 is large compared with $\eta+\varepsilon$. We can write

$$\frac{\pi}{2}\, q(a_1,\varepsilon)^2 \approx \frac{4\varepsilon}{a_1} \ .$$

Using the previous upper bound for ε, we get

$$\sigma(\omega,a_1) \approx \left(\frac{8\sqrt{2}}{\pi}\, \rho(\omega)\right)^{1/2} a_1^{-3/2} \ .$$

We expect to obtain reasonable error bounds whenever σ is small compared with $N(\hat{a}_1)$. Since

$$N(a_1) = \frac{2}{\pi a_1} \left[\sqrt{1 - \frac{\xi^2}{a_1^2}} + \sqrt{1 - \frac{\eta^2}{a_1^2}}\right] - j\, \frac{2}{\pi} \frac{(\eta-\xi)}{a_1^2} \ ,$$

We see that for sufficiently large a_1 or small $\rho(\omega)$, the error circles

(of radius σ) will be small enough to allow us to obtain a bounded set Ω for any reasonably behaved G.

For example, with a_1 near 3.5, we get $\sigma \approx 0.3\sqrt{\rho(\omega)}$. If $\xi = 0.2$ and $\eta = 1.8$, the corresponding value of $N(a_1)$ is $0.34 + j0.08$. For $\rho(\omega)$ less than about 0.35 uniformly over some range near the intersection defining a describing function solution, we will obtain $\varepsilon \leq 0.5$ and $\sigma \approx 0.18$.

The alternative to this semi-analytic approach is to work entirely numerically, using the full optimized method in Table 2. For example, with $G(s) = \frac{2.56}{s^3(s+1)^2}$, the describing function method predicts that $(\hat{\omega},\hat{a}_1) = (0.8,3.74)$ and our detailed error analysis yields $\omega \in [0.7, 0.9]$ and $a_1 \in [3.29, 3.89]$.

4. The theory

In this section we develop the new parts of the theory which justify our results. Parts of the proof of the basic theorem are virtually identical to published results, so we merely outline what is required there and give references for the details.

The theorem shows that if a bounded set Ω can be found as described in section 2, and if the non-degeneracy condition is satisfied, there is an oscillatory solution to the exact system equations. The idea behind the proof is to show that, as the describing function equations are perturbed towards the exact equations, a solution $(\dot{\omega},a_1)$ moves away from $(\hat{\omega},\hat{a}_1)$ but it can never move beyond the boundary of Ω. Indeed, no periodic solution can ever cross the boundary of Ω. The degree condition ensures that even if solutions appear or disappear (say, by mutual annihilation) there will always be at least one solution in Ω. This result, called homotopy invariance [17] is a generalization of the notion that solutions will usually only disappear by coalescing in pairs, so if we start with an odd number of non-degenerate solutions and if no solution ever crosses the boundary of Ω, there is no way in which all the solutions can be lost. The part of the proof involving degree theory is now standard and we will not be repeating it, so we do not propose to give any more technical description of degree theory: Lloyd's book [17] is exceptionally clear, and the use of degree theory in the present context is described in [10].

We now derive the expressions used to find the set Ω. The inequality for ε comes from considering an equation for neglected harmonics and the main inequality defining Ω comes from the exact equation for the first harmonic. The system equation is

$$\dot{x} = -gnx$$

and we are looking for a periodic solution $x(t)$ with period, say, $2\pi/\omega$. It is convenient to normalize time, and to write

$$\dot{x} = -g_\omega nx \tag{4.1}$$

where x has period 2π. If g has convolution kernel $\phi(t)$ then g_ω has kernel $\phi(t/\omega)/\omega$ and we see that -- not surprisingly -- $\omega > 0$ is required for continuity. If z has period 2π and has complex Fourier coefficients z_k $(k \in K)$ then $g_\omega z$ has Fourier coefficients $G(jk\omega)\ z_k$.

We work, then, on a space of 2π-periodic functions, and we choose to equip it with the L_∞ norm

$$\|z\|_\infty = \sup_{t\in[0,2\pi]} |z(t)| \ .$$

Call this space Π_∞, and let P_1 be the continuous linear operator that projects signals in Π_∞ to the first[3] harmonics and write $P^* = 1-P_1$. We can define x_1, x^*, K_1 and K^* in the obvious ways: for instance, $x^* = P^*x$ contains only harmonics whose indices are in K^*. Of course, P_1 and P^* commute with g_ω, which in plain words says that no harmonic distortion is introduced by a linear system.

We write

$$x(t) = \mathrm{Re} \sum_{k\in K} a_k\ e^{jkt}$$

so that $x_1(t) = a_1 \cos t$ with a_1 chosen to be real by adjusting the arbitrary time origin. Applying P^* and P_1 to (4.1) we get

$$\dot{x}^* = -P^*g_\omega n(x_1+x^*) \tag{4.2}$$

and

$$\dot{x}_1 = -P_1g_\omega n(x_1+x^*) \tag{4.3}$$

Using (4.3) we obtain the phasor equation

---

[3] Or zeroth and first, if we are balancing bias term too, so $K_1 = \{0,1\}$. As before, we shall lighten the notation by considering only the case where $K_1 = \{1\}$.

$$a_1 = G(j\omega)\ E(a_1,x^*)a_1 - G(j\omega)\ N(a_1)a_1 \tag{4.4}$$

where $-E(a_1,x^*)\ a_1\cos t = (P_1[n(x_1+x^*)-n(x_2)])(t)$. Since $P_1x^* = 0$ we can also write a "pole-shifted" version,

$$-E(a_1,x^*)\ a_1\cos\ t = (P_1[n(x_1+x^*)-n(x_1)-\gamma x^*])(t) \tag{4.5}$$

where γ is an arbitrary constant, which may be chosen separately for each ω and a_1. Dividing (4.4) by $G(j\omega)\ a_1$ and rearranging, we arrive at

$$N(a_1) + \frac{1}{G(j\omega)} = E(a_1,x^*) \tag{4.6}$$

which should be compared with (2.1).

At this stage, the standard method described, for example, in [6] is to apply the contraction mapping theorem to (4.2) to show that a given (ω,a_1) defines a unique x^* which varies continuously with ω and a_1, and then to write E in (4.6) as a function of ω and a_1 only. Finally, the Leray-Schauder theorem or something similar is used to bound errors in (4.6). In the present paper we are avoiding the assumption of slope bounds so we cannot obtain the Lipschitz constant needed to apply the contraction mapping theorem. Instead, we show that inequality (2.2) ensures that the right side of (4.2) maps $B(0,\varepsilon)$ into itself, where $B(0,\varepsilon)$ is the closed ball in $P^*\Pi_\infty$ of radius ε, centered at the origin. The value of ε may depend on ω and a_1. We also show that if $(\omega,a_1) \in \Omega$ and $x^* \in B(0,\varepsilon(\omega,a_1))$ then $|E(a_1,x^*)| \leq \sigma(\omega,a_1)$. If we were proving the theorem in full, we would then apply (infinite-dimensional) degree theory to (4.2) and (4.6) simultaneously, working on the space $\mathbb{R}_+^2 \times P^*\Pi_\infty$ -- or, more precisely, on the set $\{(\omega,a_1,x^*) : (\omega,a_1) \in \Omega,\ x^* \in B(0,\varepsilon(\omega,a_1))\}$. There are several technicalities concerning continuity which will be discussed briefly later.

Let us derive the inequalities. We start with (4.2), which by standard methods of pole-shifting can be converted to

$$x^* = -P^*\tilde{g}_\omega\tilde{n}(x_1+x^*)$$

with

$$\tilde{g}_\omega = (1+\gamma g_\omega)^{-1}\ g_\omega \text{ and } \tilde{n}(x) = n(x) - \gamma x$$

We write this as

$$x^* = \tilde{F}(\omega,a_1,x^*,\gamma)$$

and we derive an inequality showing that $\|x^*\|_\infty \le \varepsilon$ implies $\|\tilde{F}\|_\infty \le \varepsilon$, so that $\tilde{F}$ maps $B(0,\varepsilon)$ into itself. Now if

$$\tilde{n}(a_1 \cos t + x^*(t)) = \mathrm{Re} \sum_{k \in K} c_k e^{jkt}$$

then

$$\tilde{F}(\omega, a_1, x^*)(t) = -\mathrm{Re} \sum_{k \in K^*} \tilde{G}(jk\omega)\, c_k\, e^{jkt},$$

so by Schwartz's inequality,

$$\begin{aligned} \|\tilde{F}\|_\infty^2 &\le \sum_{k \in K^*} |\tilde{G}(jk\omega)|^2 \sum_{k \in K^*} |c_k|^2 \\ &= \tilde{\rho}(\omega,\gamma)^2 \, \|P^* \tilde{n}(x)\|_2^2 \end{aligned} \tag{4.7}$$

where $\tilde{\rho}(\omega,\gamma)^2 \triangleq \sum_{k \in K^*} |\tilde{G}(jk\omega)|^2$. At this stage, we can either set $\gamma = 0$ and use the crude bound $\|P^* n(x)\|_2 \le r(a_1,\varepsilon)$ where $r(a_1,\varepsilon)$ is defined just after (2.2), or we can try to get a better bound by writing

$$P^*(n(x) - \gamma x) = P^*(n(x) - n(x_1) - \gamma x^*) + P^* n(x_1)$$

so

$$\|P^* \tilde{n}(x)\|_2^2 \le \|n(x) - n(x_1) - \gamma x^*\|_2^2 + p(a_1)^2$$

where

$$\begin{aligned} p(a_1)^2 &= \|P^* n(a_1 \cos t)\|_2^2 \\ &= \|n(a_1 \cos t)\|_2^2 - |a_1 N(a_1)|^2 \end{aligned} \tag{4.8}$$

In (4.8) we used the Pythagorean equality on the Hilbert space H_2 of square-integrable 2π-periodic functions. Notice that as we mentioned in section 2, $p(a_1)$ is a measure of the describing function output error: the extent to which, because it neglects harmonics at the output, the describing function would be inaccurate even with a pure sinusoidal input.

For each ω and a_1 we now have

$$\begin{aligned} \|\tilde{F}\|_\infty &\le \tilde{\rho}(\omega,\gamma)(p(a_1) + \|n(x_1 + x^*) - n(x_1) - \gamma x^*\|_2) \\ &\le \tilde{\rho}(\omega,\gamma)(p(a_1) + \tilde{q}(a_1,\varepsilon,\gamma)) \end{aligned}$$

where $\tilde{q}(a_1,\varepsilon,\gamma) = \sup_{\|x^*\|_\infty \le \varepsilon} \|n(a_1\cos t + x^*(t)) - n(a_1\cos t) - \gamma x^*(t)\|_2$.

Noting the remark after (4.7) and optimizing the bound over choices of γ, we see that

$$\varepsilon \ge \min \{\min_{\gamma \in \mathbb{R}} \tilde{\rho}(\omega,\gamma)(p(a_1)+\tilde{q}(a_1,\varepsilon,\gamma)),\ \rho(\omega)\ r(a_1,\varepsilon)\} \tag{4.9}$$

ensures $\tilde{F}$ maps $B(0,\varepsilon)$ into itself. Inequality (4.9) is the same as (2.2) except that poleshifting has been allowed for. Notice that if the upper bounds on p and q mentioned in section 2 satisfy the inequality, $B(0,\varepsilon)$ will still be mapped into itself.

We have already done most of the work needed to deal with (4.6), since (4.5) gives

$$|E(a_1,x^*)| = \frac{1}{a_1} \|P_1(n(x_1+x^*) - n(x_1) - \gamma x^*)\|_2$$

$$\le \frac{1}{a_1} \tilde{q}(a_1,\varepsilon,\gamma)$$

which, on minimizing over γ, gives $\sigma(\omega,a_1)$ as defined in (2.4).

Observe that all of the above works perfectly well for "multivalued" nonlinear elements such as hysteresis or backlash since N, p and r are always well-defined and q is well-defined if ε is not too large. The reason there is no difficulty is that such elements induce single-valued maps on spaces of periodic functions provided the initial state is consistent with periodic behavior.

The main technical issue which we do not discuss in detail here is that degree theory, on which the theorem relies, only works if all functions are <u>continuous</u>; and in fact g_ω has to be completely continuous (compact), which is a restriction following automatically from the low-pass condition implied by finiteness of $\rho(\omega)$. Most of the continuity analysis is routine, but if $n(\cdot)$ is discontinuous there is an added difficulty. The technique used in [8] overcomes this difficulty. There, Michel and Miller have shown that if n is discontinuous, but if there exists a set Ω which works for all sufficiently good continuous approximations to n, it is possible to define <u>weak solutions</u>. We say the system has a weak periodic solution x if n is the limit of a sequence of slope-bounded relations $\{n_k\}$ having periodic solutions $\{x_k\}$, and $x_k \to x$ as $k \to \infty$. From the practical point of view, there is nothing to check except that

such a sequence $\{n_k\}$ could exist and would result in $\{p_k\}$, $\{q_k\}$, $\{r_k\}$ and $\{N_k\}$ which converge to p, q, r and N. This is true of all nonlinear elements that, over the domain $[a_1^m-\varepsilon, a_1^m+\varepsilon]$ where $a_1^m = \sup_\Omega a_1$, consist of a finite number of Lipschitz continuous segments, with the usual hysteresis or backlash rules for choosing the correct segment whenever segments overlap. Let us call this set of elements *N*.

Theorem 4.1.

For the feedback system of Fig. 1.1, suppose $n \in N$ and there exists a closed subset Ω of $(\omega>0, a_1>0)$ such that for all $(\omega,a_1) \in \Omega$,

$$|N(a_1)+1/G(j\omega)| \leq \sigma(\omega,a_1) \quad .$$

If Ω is bounded and $d(N+1/G,\Omega,0) \neq 0$ then the equation $z = -gnz$ has a periodic solution $z(t) = x(\omega t)$ where

$$x(\omega t) = a_1 \cos \omega t + x^*(\omega t)$$

for some $(\omega,a_1) \in \Omega$ and $x^* \in P^*\pi_\infty$ with $\|x^*\|_\infty \leq \varepsilon$, where $\varepsilon = \sup_\Omega \varepsilon(\omega,a_1)$ and $\varepsilon(\omega,a_1)$ is defined by (4.9).

Outline of Proof

When n is continuous as a map from Π_∞ to Π_∞, the proof is virtually identical to that of Theorem 5.2.15 in reference [10], with the new error bounds and the simplifying assumptions that x is scalar and there is only one harmonic to be balanced. Applying Michel and Miller's work in [8] on weak solutions, the same result can be obtained when n is discontinuous. The interested reader should consult these publications for details.

Acknowledgements

The authors would like to thank Mr. David Carter of the Department of Control and Management Systems, Cambridge University, for having written computer programs based on an earlier version of the paper.

References

[1] Bass, R. W., Proc. IFAC Moscow 1960, p. 895

[2] Cesari, L., "Functional analysis, nonlinear differential equations, and the alternative method," in L. Cesari, R. Kannan and J. Schuur (Eds), Nonlinear Functional Analysis and Differential Equations, Dekker, New York 1976.

[3] Kudrewicz, J., "Theorems on the existence of periodic vibrations based upon the describing function method," Proc. IFAC, Warsaw, Paper 4.1, p. 46, 1976.

[4] Bergen, A. R. and Franks, R. L., "Justification of the describing function method," SIAM J. Control, vol. 9 (4), 568-589, 1971.

[5] Mees, A. I., "The describing function matrix," J. Inst. Maths. Applics., vol. 10, 49-67, 1972.

[6] Mees, A. I. and Bergen, A. R., "Describing functions revisited," IEEE Trans. Automatic Control, vol. AC-20 (4), 473-478, 1975.

[7] Williamson, D., "Periodic motion in nonlinear systems," IEEE Trans. Automatic Control, vol. AC-20 (4), 479-486, 1975.

[8] Michel, A. N. and Miller, R. K., "On existence of periodic motions in nonlinear control systems with periodic inputs," presented at the JACC, San Francisco, August, 1980.

[9] Blackmore, D., "The describing function for bounded nonlinearities," IEEE Trans. on Circuits and Systems, vol. CAS-28 (5), May, 1981.

[10] Mees, A. I., Dynamics of Feedback Systems, John Wiley and Sons Ltd., London, 1981.

[11] Gelb, A. and Vander Velde, W. E., Multiple-input Describing Functions and Nonlinear System Design, McGraw Hill Inc., NY 1968.

[12] Krasnosel'skiy, M., Perov, A. I., Povolotskiy, A. I., Zabreiko, P. P., Plane Vector Fields, Academic Press, NY 1966.

[13] Chua, L. O. and Wang, N. N., "On the application of degree theory to the analysis of resistive nonlinear networks," International Journal of Circuit Theory and Applications, vol. 5, 1977, pp. 35-68.

[14] Avriel, M., Nonlinear Programming Analysis and Methods, Prentice-Hall Inc., New Jersey, 1976.

[15] Ogata, K., Modern Control Engineering, Prentice-Hall Inc., New Jersey, 1970.

[16] Mees, A. I. and Chua, L. O., "The Hopf bifurcation theorem and its applications to nonlinear oscillations in circuits and systems," IEEE Trans. on Circuits and Systems, vol. CAS-26 (4), April, 1979,

[17] Lloyd, N., Degree Theory, Cambridge University Press, London, 1978.

Table 1. Summary of simple error bound calculation

(We assume that n is a single-valued odd function and is monotone increasing or decreasing; we only look for solutions composed of odd harmonics. Table 2 deals with the general case and also gives tighter bounds than in the present case.)

Step	Description
0	Find $(\hat{\omega},\hat{a}_1)$ satisfying $N(\hat{a}_1) + \frac{1}{G(j\hat{\omega})} = 0$. Check that the N and -1/G loci are not parallel where they intersect at $(\hat{\omega},\hat{a}_1)$.
1.	Let $\rho(\omega)^2 = \sum_{k=3,5,\ldots} \lvert G(jk\omega)\rvert^2$.
2.	Let $p(a_1) = \lVert n(a_1 \cos t)\rVert_2^2 - \lvert a_1 N(a_1)\rvert^2$. (If n has gain β, we can use $p(a_1) \leq \beta a_1$.)
3.	Let $q(a_1,\varepsilon) = \lVert m(a_1 \cos t, \varepsilon)\rVert_2$ where $m(x,\varepsilon) = \max\{\lvert n(x+\varepsilon)-n(x)\rvert, \lvert n(x-\varepsilon)-n(x)\rvert\}$ (If n has slope bound λ, we can use $q(a_1,\varepsilon) \leq \sqrt{2}\,\lambda\varepsilon$)
4.	Choose ε such that for all (ω,a_1) near $(\hat{\omega},\hat{a}_1)$, $\varepsilon \geq \rho(\omega)(p(a_1)+q(a_1,\varepsilon))$.
5.	Find the set Ω of (ω,a_1) values near $(\hat{\omega},\hat{a}_1)$ such that $\lvert N(a_1) + \frac{1}{G(j\omega)}\rvert \leq q(a_1,\varepsilon)/a_1$. (This can be done graphically: see the text.) Check that Ω is bounded.
6.	Check that Ω only contains the one describing function solution $(\hat{\omega},\hat{a}_1)$.
7.	There is at least one true periodic solution with $(\omega,a_1) \in \Omega$ and $\lVert x^*\rVert_\infty \leq \varepsilon$.

Table 2. Summary of general error bound calculation

(Not all the optimizations need be carried out; for example, γ can be set to 0 everywhere.)

Step	Description
0	Find all $(\hat{\omega},\hat{a}_1)$ satisfying $N(\hat{a}_1) + \frac{1}{G(j\hat{\omega})} = 0$, where N accounts for the zero'th harmonic if relevant.
1.	Let $K = \{1,3,5...\}$ (or $\{0,1,2,3...\}$ if even harmonics are allowed,) and $K^* = K\backslash\{1\}$ (or $K\backslash\{0,1\}$ if the zero'th harmonic has been balanced).
2.	Let $\tilde{\rho}(\omega,\gamma)^2 = \sum_{k\in K^*} \lvert G(jk\omega)/(1+\gamma G(jk\omega))\rvert^2$.
3.	Let $p(a_1)^2 = \lVert n(a_1\cos t)\rVert_2^2 - \lvert a_1 N(a_1)\rvert^2$.
4.	Let $\tilde{q}(a_1,\varepsilon,\gamma) = \sup_{\lVert x^*\rVert_\infty \le \varepsilon} \lVert n(a_1\cos t + x^*) - n(a_1\cos t) - \gamma x^*\rVert_2$ Denote $q(a_1,\varepsilon) = \min_\gamma \tilde{q}(a_1,\varepsilon,\gamma)$
5.	Let $r(a_1,\varepsilon) = \sqrt{2} \sup_{\lvert y\rvert \le a_1+\varepsilon} \lvert n(y)\rvert$, and for each (ω,a_1,γ), find the smallest positive solution of $\varepsilon(\omega,a_1,\gamma)$ of $\varepsilon = \tilde{\rho}(\omega,\gamma)\min\{\tilde{q}(a_1,\varepsilon,\gamma) + p(a_1),\ r(a_1,\varepsilon)\}$. For each (ω,a_1) let $\varepsilon(\omega,a_1) = \min_\gamma \varepsilon(\omega,a_1,\gamma)$.
6.	Choose a solution $(\hat{\omega},\hat{a}_1)$ and find the smallest connected component Ω of $\{(\omega,a_1) : \lvert N(a_1) + 1/G(j\omega)\rvert \le q(a_1,\varepsilon(\omega,a_1),a_1)/a_1\}$ containing $(\hat{\omega},\hat{a}_1)$
7.	Check that the degree $d(N+\frac{1}{G},\Omega,0)$ is nonzero.
8.	There is at least one true periodic solution with $(\omega,a_1) \in \Omega$ and $\lVert x^*\rVert_\infty \le \varepsilon$.

Figure Captions

Figure 1.1. Autonomous single-loop feedback system studied in the paper.

Figure 2.1. Error discs used in locating the set Ω, in which the exact solution lies.

Figure 2.2. The degree in (a), (b) and (c) is nonzero because the intersection cannot be removed by perturbation; but the degree in (d) is zero.

Figure 3.1. Backlash nonlinearity of Example 3.1.

Figure 3.2. Error circles for Example 3.1.

Figure 3.3a. The Wien bridge oscillator of Example 3.2.

Figure 3.3b. Ideal Operational Amplifier characteristic

Figure 3.4. Poleshifting the nonlinearity in Example 3.2 to obtain a strictly proper $G'(s)$.

Figure 3.5. Saturation characteristic

Figure 3.6. Nyquist locus of Example 3.3.

Figure 3.7. Region Ω containing the exact solution in Example 3.3.

Figure 3.8. Hysteretic relay of Example 3.4

Table Captions

Table 1. Summary of simple error bound calculation.

Table 2. Summary of general error bound calculation.

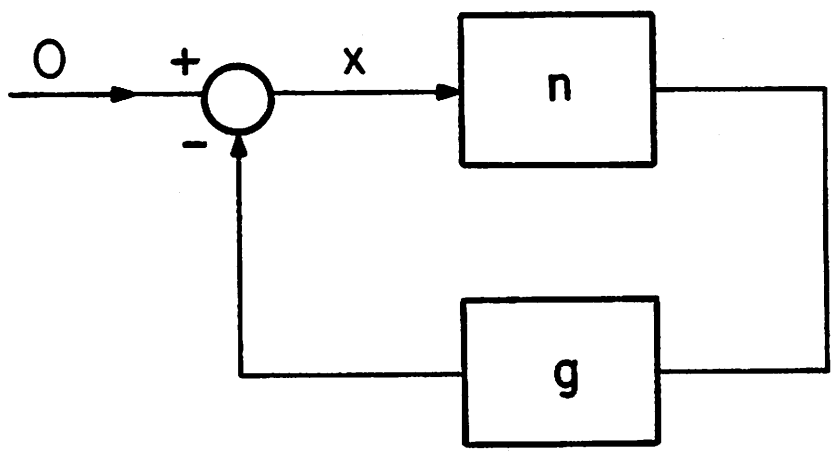

Fig. 1.1

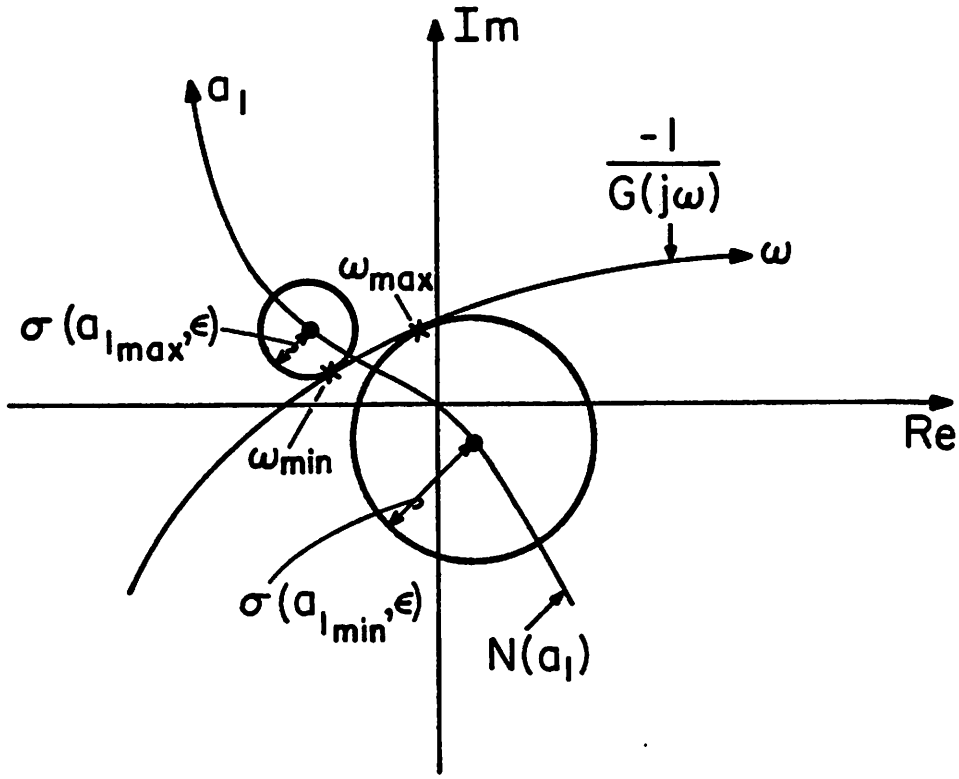
Im
a_1
$\frac{-1}{G(j\omega)}$
ω
ω_{max}
$\sigma(a_{1max},\epsilon)$
Re
ω_{min}
$\sigma(a_{1min},\epsilon)$
$N(a_1)$

Fig. 2.1

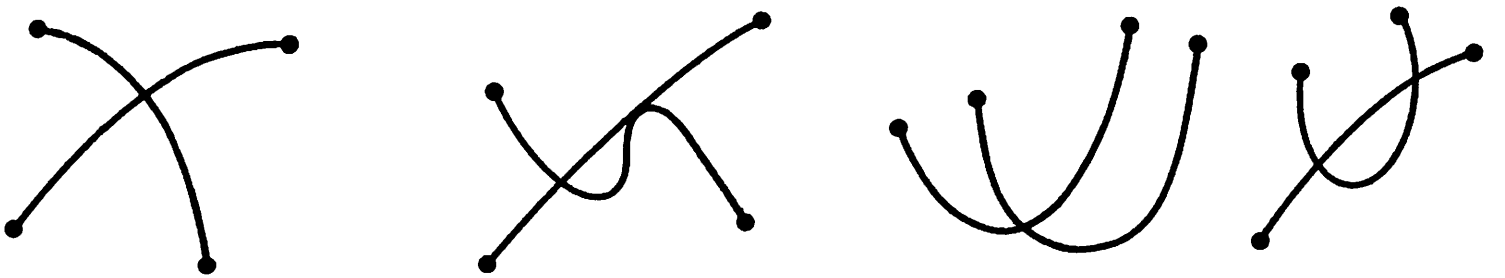

Fig. 2.2

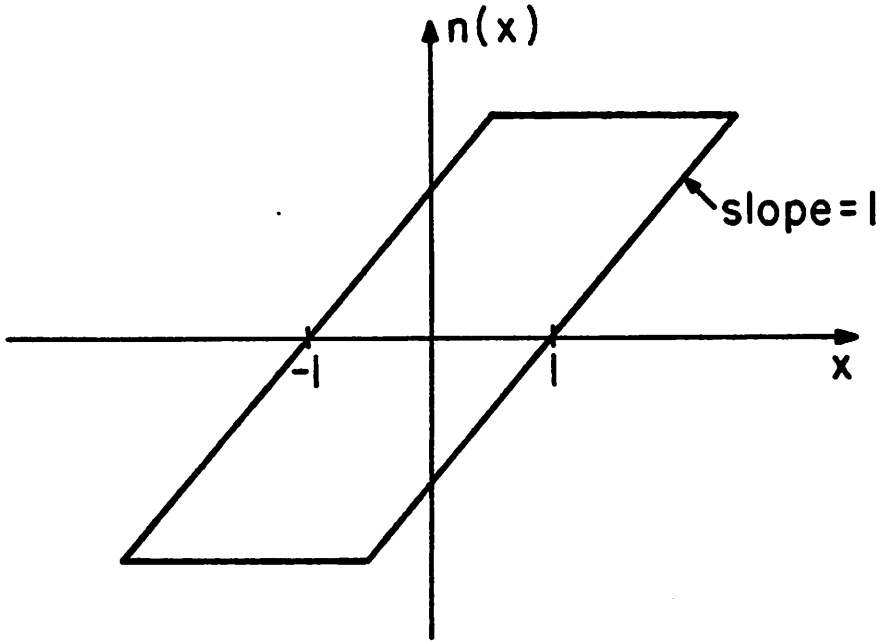

Fig. 3.1

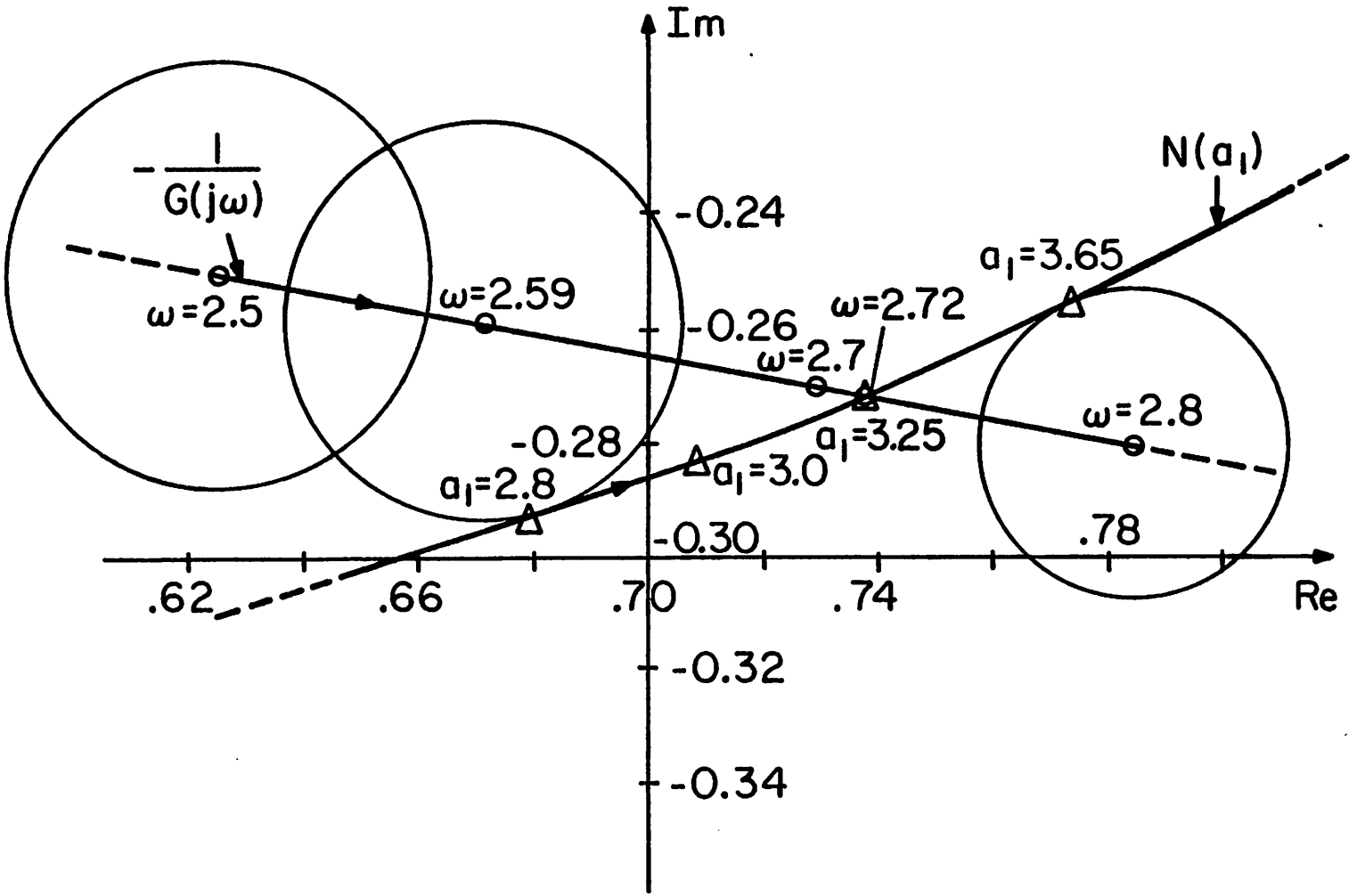
Im
$-\frac{1}{G(j\omega)}$
N(a_1)
-0.24
-0.26
-0.28
-0.30
-0.32
-0.34
a_1=3.65
ω=2.72
ω=2.59
ω=2.5
ω=2.7
ω=2.8
a_1=3.25
a_1=3.0
a_1=2.8
.62
.66
.70
.74
.78
Re

Fig. 3.2

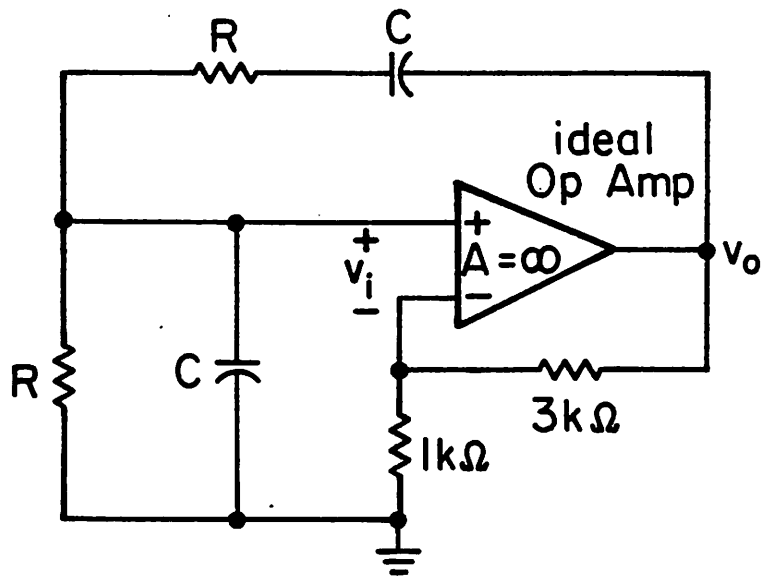

(a)

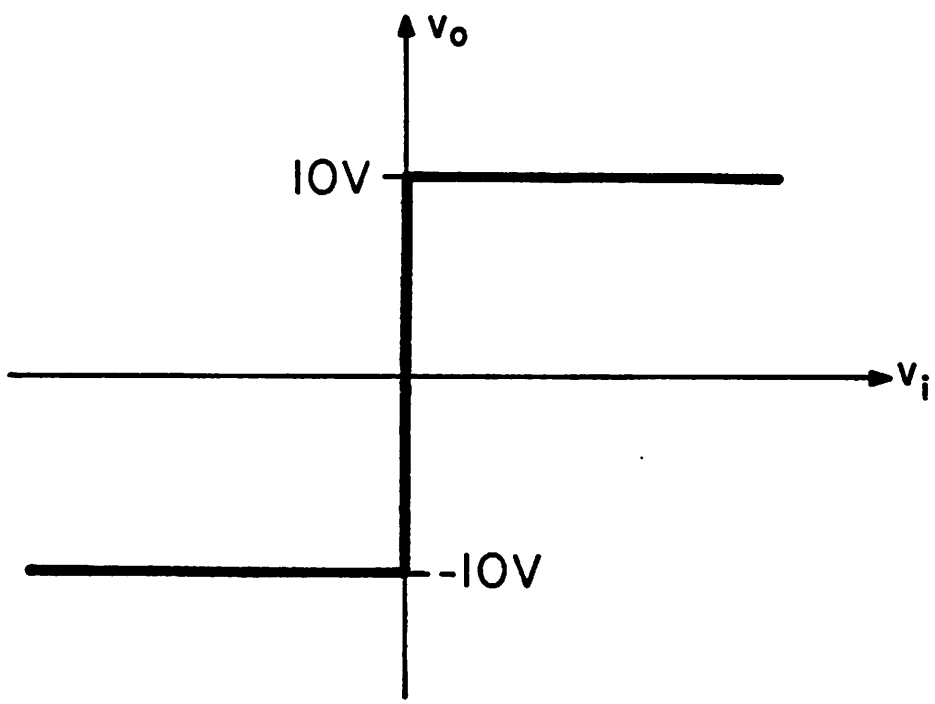

(b)

Fig. 3.3

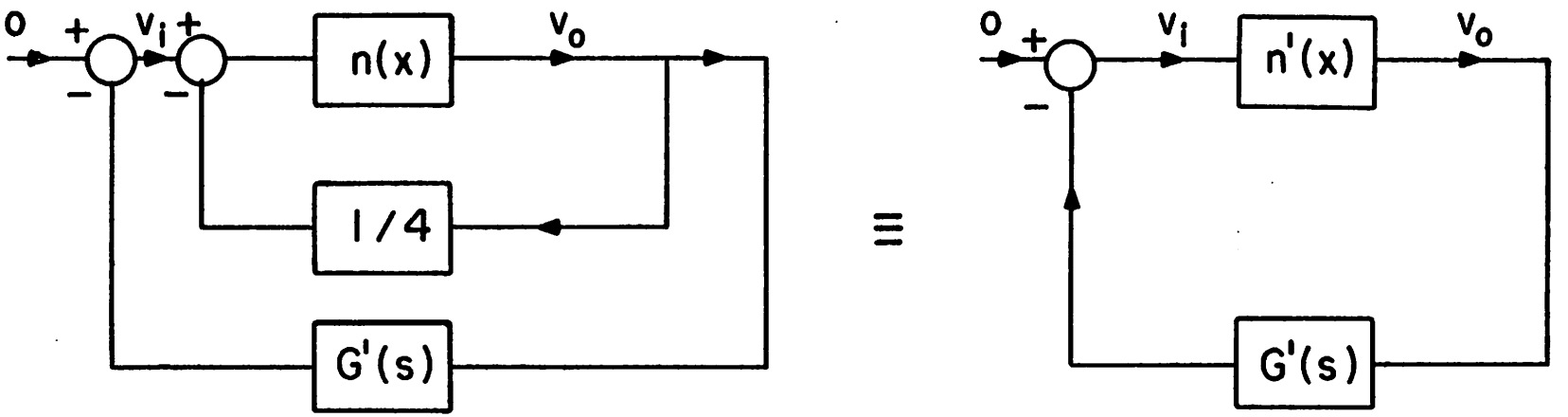

$$G'(s) = \frac{-s}{s^2+3s+1}$$

Fig. 3.4

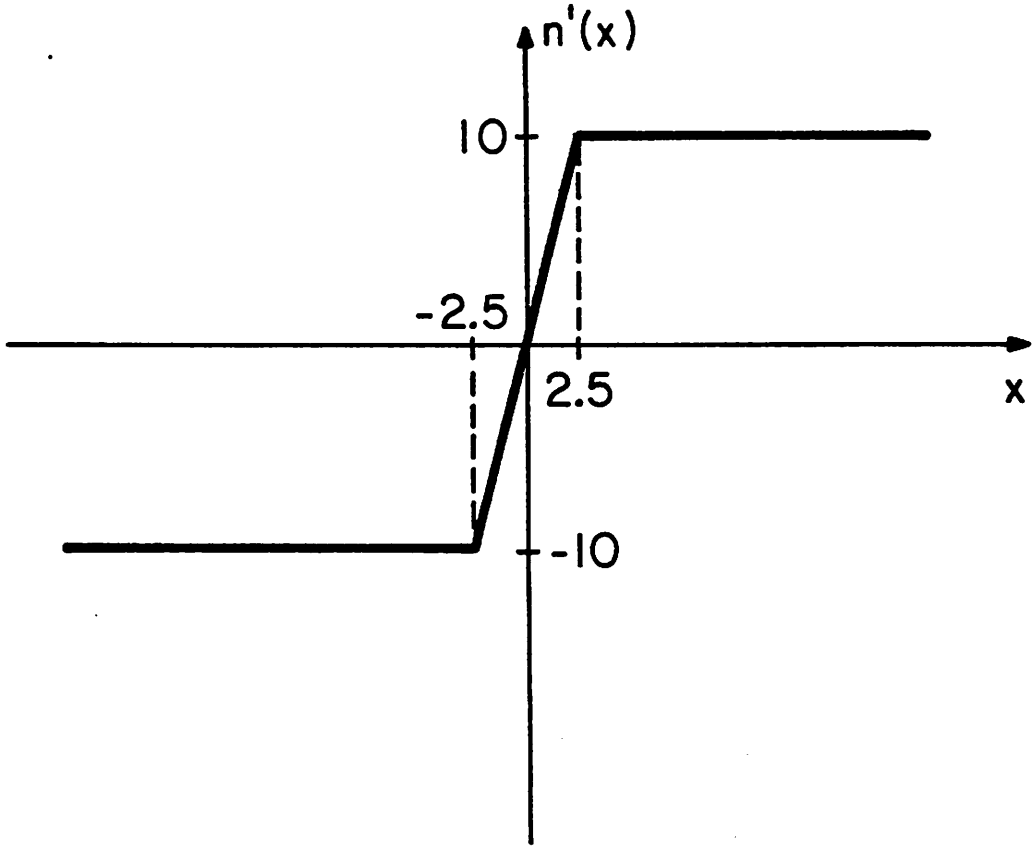

Fig. 3.5

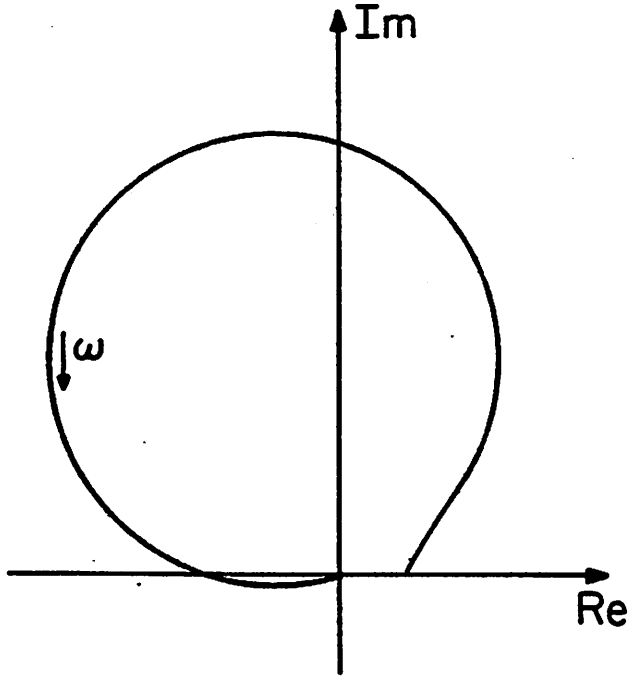

Fig. 3.6

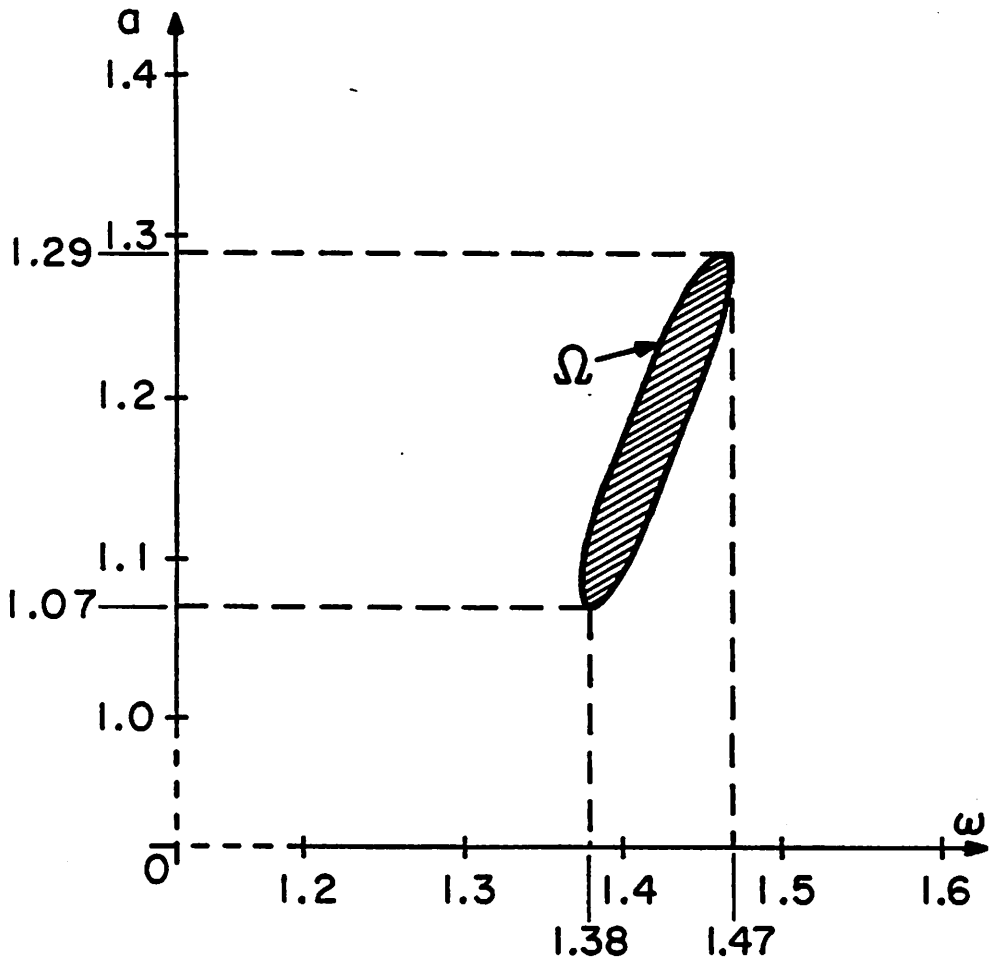

Fig. 3.7

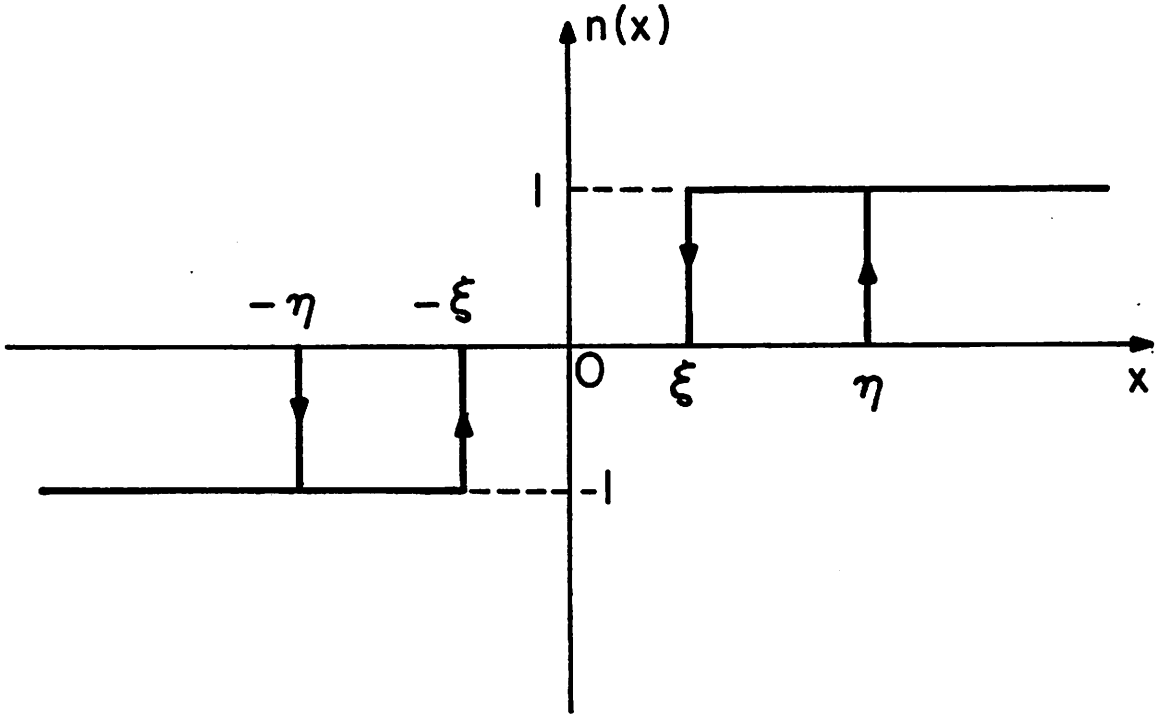

Fig. 3.8